Scientific Research Publishing

Journal of Power and Energy Engineering, 2024, 12, 23-38
https://www.scirp.org/journal/jpee
ISSN Online: 2327-5901
ISSN Print: 2327-588X

Optimal Sizing and Power Losses Reduction of Photovoltaic Systems Using PVsyst Software

Andre Boussaibo[1*], Armel Duvalier Pene[1], Kitmo[2]

[1]Institute of Technology, University of Ngaoundere, Ngaoundere, Cameroon
[2]National Advanced School of Engineering of Maroua, University of Maroua, Maroua, Cameroon
Email: *boussaibo@yahoo.fr

How to cite this paper: Boussaibo, A., Pene, A.D. and Kitmo (2024) Optimal Sizing and Power Losses Reduction of Photovoltaic Systems Using PVsyst Software. *Journal of Power and Energy Engineering*, **12**, 23-38.
https://doi.org/10.4236/jpee.2024.127002

Received: June 25, 2024
Accepted: July 23, 2024
Published: July 26, 2024

Copyright © 2024 by author(s) and Scientific Research Publishing Inc.
This work is licensed under the Creative Commons Attribution International License (CC BY 4.0).
http://creativecommons.org/licenses/by/4.0/

Open Access

Abstract

This paper presents a method for optimizing a grid-connected photovoltaic system through an LCL filter. An algorithm based on particle swarm optimization (PSO) is used to determine the number of batteries, the number of panels in series and in parallel, as well as to evaluate the joule losses due to cable heating and the switching losses of the multilevel inverters. This system is applied to a village named YAGOUA, located in the far north of Cameroon. The evaluation of the Joule effect and the switching losses as well as the regulation of the voltage level at the point of common coupling (PCC) are carried out in PVsyst and Matlab software, then at IEEE 33 bus. This algorithm reduced the Joule losses to 1.2% and the switching losses to 2.2%. A power of 210.4 MWh is produced, to be injected in the electrical network via an LCL filter. The THD calculation gave a rate of 3.015% in accordance with the 519 standards. Synchronization through the Phase Locked Loop (PLL) is performed. After the power was injected into the grid, the voltage and current remained in phase, showing the power factor correction and the efficiency of the filter. According to NASA meteorological data, the locality of YAGOUA gives the global solar irradiation forecast of 6.8 kW/m^2.

Keywords

Five Level Inverter, LCL Filter, MPPT, Power Losses, PVsyst

1. Introduction

Most of the problems encountered in industrial and domestic installations are due to the presence of odd harmonics generated either by the poor modulation technique of static converters or by non-linear loads. With the increasing progress in power electronics [1]-[3], optimization and safety of installations

must be a necessity. The presence of harmonics causes losses or heating on electrical installations [4]. In the literature, several methods have been developed in order to minimize or even eliminate these disturbing quantities, which deteriorate the components of power electronics and cause energy losses [5]-[7]. Examples are active filtering [4], MPPT control or metaheuristic techniques [8]. In this paper, we have developed an optimization technique by eliminating odd harmonics, up to rank 21, using a MPPT control of the PSO and PLL synchronization [9]-[11]. This model is a solution to the needs and problems encountered by industries and homes in terms of the quality of energy transmitted to the receivers. Simulation results in this study are done in Matlab/Simulink and PSIM software is used for the modeling of the system.

2. Materials and Methods

2.1. Diagram of the PV System

This control system is located upstream of the five-stage inverters in **Figure 1**.

2.2. PV Generator Current

The Equation (1) is the mathematical expression of the current produced by the PV generator. For the simulation of the PV system, this equation is modeled by Simulink blocks.

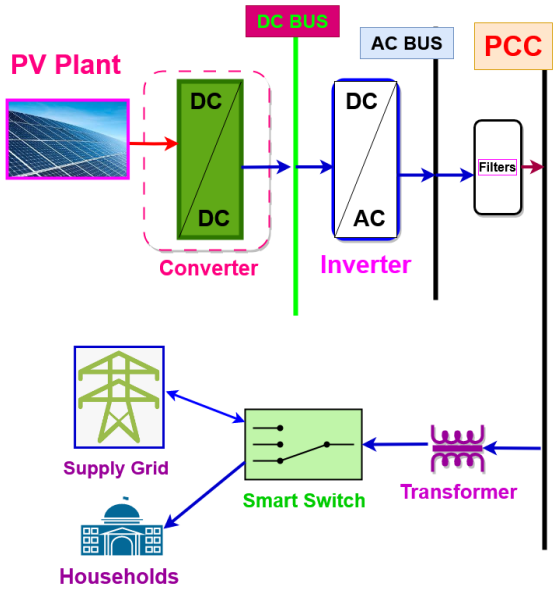

Figure 1. PV system overview diagram.

$$I = N_p I_{ph} - N_p I_o \left[\exp\left(\frac{q\left(N_s V + \left(\frac{N_s}{N_p} \right) R_s I \right)}{N_s nKT} \right) - 1 \right] - \frac{q\left(N_s V + \left(\frac{N_s}{N_p} \right) R_s I \right)}{\left(\frac{N_s}{N_p} \right) R_{sh}} \quad (1)$$

where:

I: Cell Output Current (A)

V: Operating Voltage (V).

K: Boltzmann constant (13805-10-23 Nm/˚K)

N_P: Number of cells in parallel

I_{PH}: Photocurrent (A)

I_o: Saturation current of the diode (A)

R_S: Series Resistance of Cell (Ω)

N_S: Number of cells in series

R_{sh}: Shunt Resistance of Cell (Ω)

n: Ideality Factor

Table 1 below summarizes the characteristics of the photovoltaic panel necessary for the simulation of the simulink model of the photovoltaic generator.

Table 1. Photovoltaic panel characteristics.

Characteristics	Reference	Values
Type	polycristalline	
Maximum power	P_m	47.08 W
Maximum voltage	V_{mp}	26.56 V
Maximum current	I_{mp}	8.25 A
Open circuit voltage	V_{oc}	21.6 V
Open circuit current	I_{scr}	4.55 A
Temperature range	−40˚C à +85˚C	
Number of cells in series	N_s	70
Number of cells in parallel	N_p	14

2.3. The Boost Chopper

Sunshine is a random quantity, that is to say non-linear. In order to improve the quality of the electrical from photovoltaic generator, it is necessary to use boost chopper of Figure 2. It is a static converter of continuous-to-continuous quantities. Its duty cycle is controlled by the MPPT controller who's the algorithm is illustrated in Figure 2.

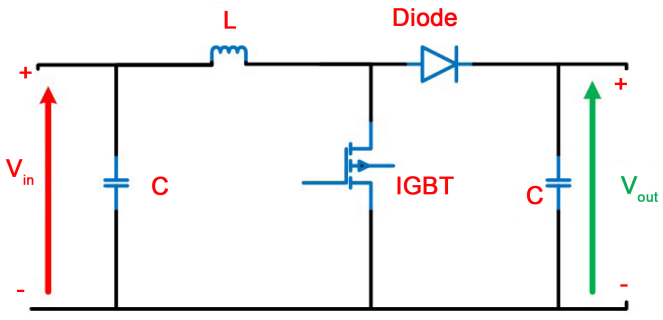

Figure 2. Model of the Boost converter.

The Maximum Power Point tracking algorithm is an optimization technique that extracts the maximum power generated by a given signal [12]-[14]. The technique use in this study differs from the classical algorithm [8] in the fact that, it is based on a modified PSO model.

The technique allows the current generated by the photovoltaic generators to maintain the upper extremum. The flowchart is depicted in **Figure 3**.

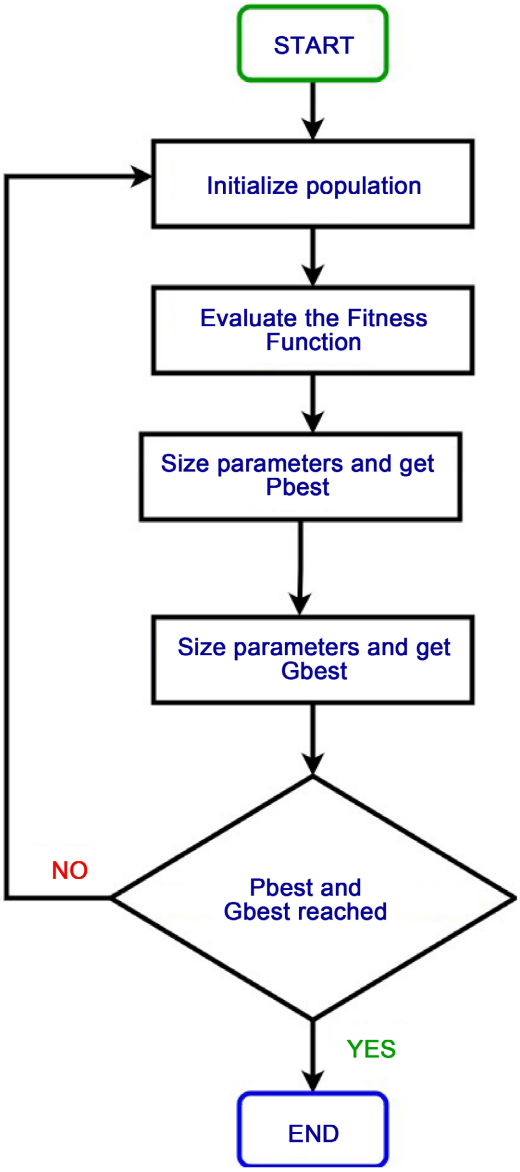

Figure 3. Flowchart of the PSO Algorithm.

2.4. Choice of Inverter

The multilevel inverters that we have used are inverters with five cascaded levels in **Figure 4**, unlike the NPN inverters or inverters with floating bus voltages which pose the problems of voltage balance [5] or even the problems of switching losses and losses by Joule effect.

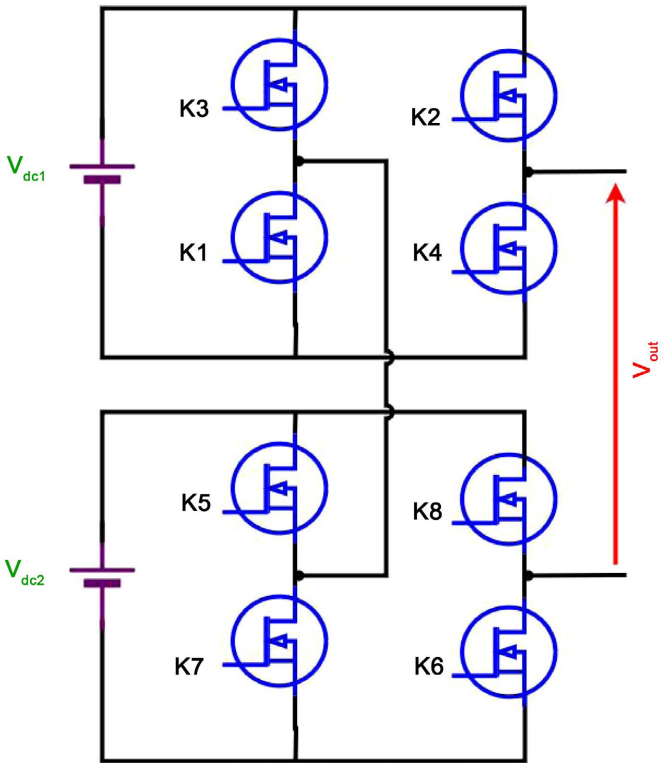

Figure 4. Control unit for complementary arms.

2.5. Triangular Sine PWM

Sine-triangular modulation consists of using n-1 triangular carriers of the same amplitude for a level n [15]. The modulation of a five-level inverter technique is depicted in **Figure 5**.

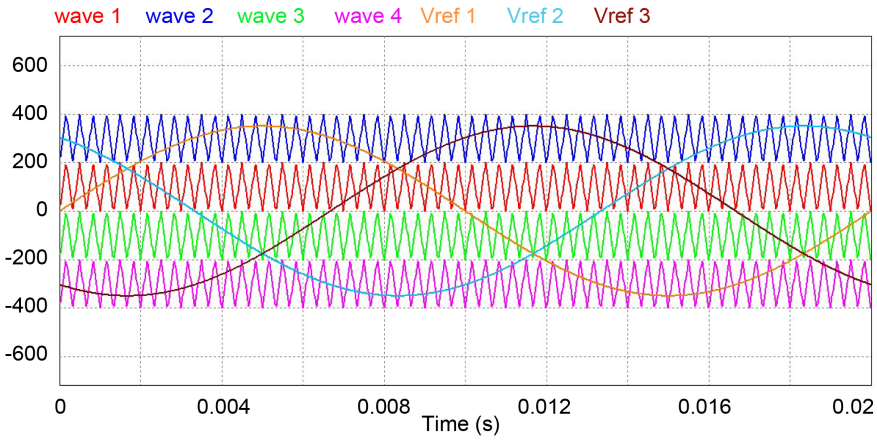

Figure 5. Triangulo sine modulation with four carriers.

The modulation of multilevel inverters the most used in the literature is that known as triangulo-sinusoidal [16] [17] where the arms of each switching cell are complementary to each other two by two. **Figure 6** represents a switching cell.

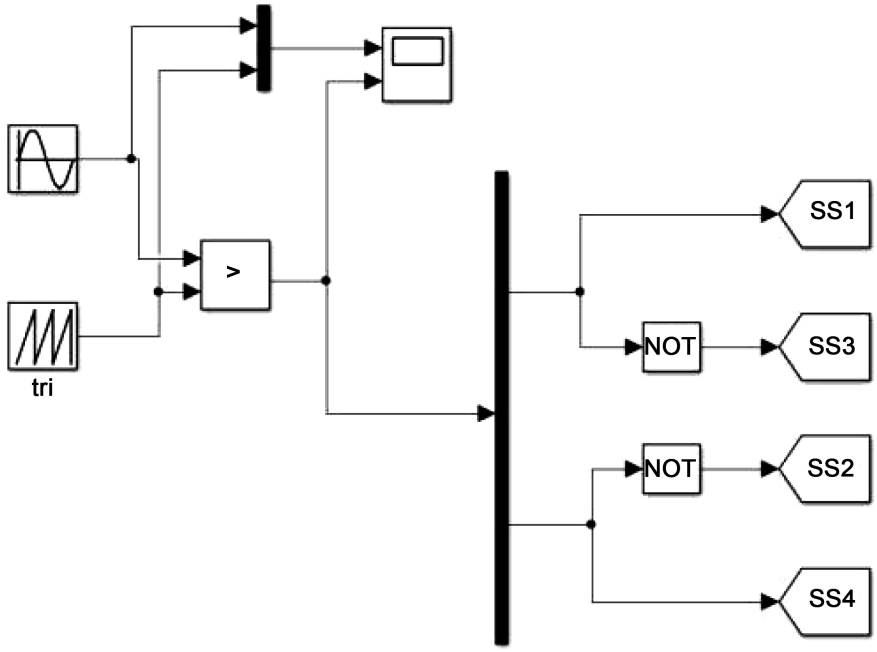

Figure 6. Control unit for complementary arms.

2.6. Diagram of the First Order LCL Filter

The diagram in Figure 7 below is the LCL filter used in this work. It is a first order filter. Its role is to extract the perfectly sinusoidal signal with a frequency of 50 Hz from the signal resulting from the DC/AC conversion.

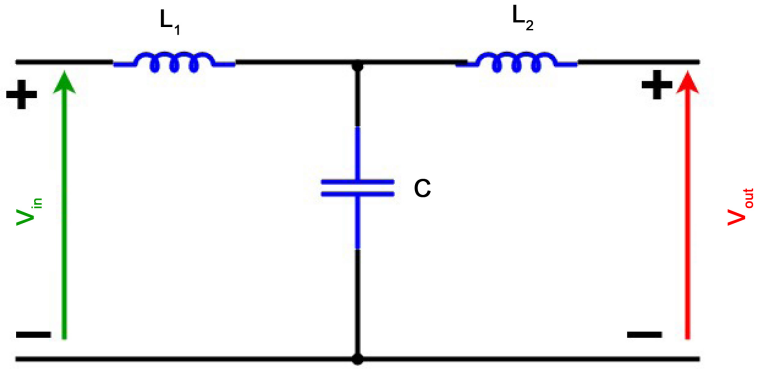

Figure 7. Model of the LCL filter.

2.7. Load Profile

To apply PLL synchronization, we are required to make a three-phase to two-phase transformation [18]. The mathematical equations of these transformation models are given in Equations (2) (4) and (6) [19].

The reference voltages are the output voltages of the five-level inverters. It is these voltages that undergo the Park transformation known as three-phase two-phase and are controlled and injected into the power grids. In this, the electrical networks constitute the load.

$$\begin{cases} V_a = V_m \cos(\theta) \\ V_b = V_m \cos(\theta - \gamma) \\ V_c = V_m \cos(\theta + \gamma) \end{cases} \tag{2}$$

$$\begin{bmatrix} V_\alpha \\ V_\beta \end{bmatrix} = \frac{2}{3} \begin{bmatrix} 1 & -\frac{1}{2} & -\frac{1}{2} \\ 0 & \frac{\sqrt{3}}{2} & -\frac{\sqrt{3}}{2} \end{bmatrix} . \begin{bmatrix} V_a \\ V_b \\ V_c \end{bmatrix} \tag{3}$$

$$\begin{bmatrix} V_d \\ V_a \end{bmatrix} = \begin{bmatrix} \cos(\theta) & \sin(\theta) \\ -\sin(\theta) & \cos(\theta) \end{bmatrix} . \begin{bmatrix} V_\alpha \\ V_\beta \end{bmatrix} \tag{4}$$

V_d and V_a are two-phase components and V_a, V_b, V_c are three-phase voltages assumed to be balanced before the injection of the harmonic quantities from the PVG. They are out of phase with each other by an angle of $\gamma = \frac{2\pi}{3}$.

$$\begin{bmatrix} V_d \\ V_q \end{bmatrix} = \frac{2}{3} \begin{bmatrix} \cos(\theta) & \cos(\theta - \gamma) & \cos(\theta + \gamma) \\ -\sin(\theta) & -\sin(\theta - \gamma) & -\sin(\theta + \gamma) \end{bmatrix} . \begin{bmatrix} V_a \\ V_b \\ V_c \end{bmatrix} \tag{5}$$

When $V_a + V_b + V_c = 0$, for a balanced three-phase system, the identification of the harmonics is made thanks to Park's reverse voltages of the following equation's system:

$$\begin{bmatrix} V_a \\ V_b \\ V_c \end{bmatrix} = \begin{bmatrix} \cos(\theta) & -\sin(\theta) \\ \cos(\theta - \gamma) & -\sin(\theta - \gamma) \\ \cos(\theta + \gamma) & -\sin(\theta + \gamma) \end{bmatrix} . \begin{bmatrix} V_d \\ V_q \end{bmatrix} \tag{6}$$

We can define the THD as follow [18]:

$$\mathrm{TDH}(\%) = 100 \sqrt{\sum_{i=2}^{n=\infty} \frac{V_h^2}{V_1^2}} \tag{7}$$

V_h: represents the harmonic component of rank *h*.

V_1: represents the fundamental component.

2.8. Particle Swarm Optimization

Particle swarm optimization is an evolutionary algorithm that uses a population of candidate solutions to develop an optimal solution to the problem. This algorithm was proposed by Russel Eberhart and James Kennedy (Kennedy and Eberhart, 1995). He was originally inspired by the living world, more precisely by behavior of animal living in swarms, flights groups of birds. Indeed, we can observe in these animals' movement dynamics relatively complex, whereas individually each individual has "intelligence" limited, and has only local knowledge of her situation in the swarm. Local information and the memory of each individual are used to decide their shifting. Simple rules, such as "stay close to other people", "go in the same direction" or "going at the same speed", sufficient to maintain cohesion of the swarm, and allow the implementation of complex collective behaviors and adaptation. The particle swarm is a population of simple

agents called particles. Each particle is considered as a solution of problem, where it has a position (the solution vector) and a speed. In addition, each particle has a memory allowing him to remember his best performance (in position and in value) and the best performance achieved by the "neighboring" particles (informants): each particle has in fact a group of informants, historically called its neighborhood. Each individual in PSO represents a possible solution assumed to have two properties: velocity and position. Each particle wanders through in the solution area and recalls the best functional objective value (position), which has already been discovered; the fitness value is saved and known Pbest. When a particle captures all the best population as its topological neighbors, the superior value is a global best and it is called Gbest. The particles flight with a certain velocity in the D-dimensional space to find the optimal solution. Let the variable (x_i) refers to the position of particle (i) in the study space and its speed is (v_i), so the (i_{th}) from the particle can be represented as (Lu *et al*., 2015):

$$X_i = \left[X_{i1}, X_{i2}, X_{i3}, \cdots, X_{iD}\right] \tag{8}$$

The best past position of the i_{th} particle is saved under the name vector and calculated by:

$$P_i = \left(P_{i1}, P_{i2}, \cdots, P_{iD}\right)$$

where $i = 1, 2, 3, \cdots, N$ is the number of particles in a swarm:

$$v_i(t+1) = w(t)v_i(t) + c_1 r_1\left(P_i(t) - X_i(t)\right) + c_2 r_2\left(G(t) - X(t)\right) \tag{9}$$

The r_1 and r_2 are random real numbers drawn from [0, 1]; c_1 and c_2 are acceleration constants that pull each particle towards. Initialization of parameter: population size:

(N_{Pop}) = 200; c_1 = 2; c_2 = 2 and X = 0.7, total number of iterations = 100.

The procedure for the implemented PSO is as the following:

1) Set PSO parameters

Number of particules (N_P) = 200;

Population size (N_{Pop}) = 200,

Inertia weight (w) = 0.5,

Inertia weight damping ratio (w_{damp}) = 0.99, personal learning coefficient (c_1) = 2,

Global learning coefficient (c_2) = 2,

Total number of iterations = 100.

Number of variable (n_{var}) = 4;

For i = 1:N_P

2) Set dimension of the search variables

N_{PV}: number of panels,

N_{Bat}: number of batteries;

n: number of households

$$\begin{cases} N_{PV} \geq 0 \\ N_{Bat} \geq 0 \\ N \geq 0 \end{cases}$$

3) Initialization

$$X_i = \left[N_{PV}, N_{Bat}, N_n\right],\ V_i = 0$$

4) Fitness of particle

$$P_{best_i} = X_i$$

End

5) $K = 0$; while $k \leq$ max of number of iterations

6) Update velocity and position of particles

$$v_i(t+1) = w(t)v_i(t) + c_1r_1\left(P_i(t) - X_i(t)\right) + c_2r_2\left(G(t) - X(t)\right),\quad X_i^{k+1} = X_i^k + V_i^{k+1}$$

7) Evaluate the fitness function

If $k <$ max iteration,

Then $k = k + 1$ and go to step 5

Else go to step 7

We have three functional objectives:

$$\begin{aligned}\text{Object } 1 &= \min f\left(N_{PV}, N_{WT}, E_{ESS}\right)\\ &= N_{PV}\cdot C_{PV} + N_{WT}\cdot C_{WT} + C_{ESS}\cdot E_{ESS}\\ PVC_{tot} &= PVC_{PV} + PVC_{Bat}\end{aligned}$$

2.9. Constraints

A condition is given on the energy management of the solar panel array and the number of panels in Equation (10). Equation (11) defines the charging and discharging interval of the battery banks, while Equation (12) defines the energy management of the solar array and the energy stored in the batteries for injection into the power grid or for non-linear loads. This equation is applied for solar power that is sufficient to supply the electricity grids. The batteries are recharged as the system achieves steady state.

- PV power limits:

$$P_{pv\min} \leq P_{pv}(t) \leq P_{pv\max};\quad N_{pv} \geq 0 \tag{10}$$

- ESS stored energy and power limits:

$$E_{ESS\min} \leq E_{ESS}(t) \leq E_{ESS\max} \tag{11}$$

$$E_{ESS\min} = (1 - DOD)\cdot E_{ESS\max}$$

- Power balance

$$P_{pv}(t) \pm P_{ESS}(t) \geq P_{load}(t) \tag{12}$$

3. Results

3.1. Synchronization Using PLL

Synchronization by PLL illustrated in **Figure 8** allows us to have the I_d, and I_q currents which follow the PI command order, and quickly catch up with the reference quantities I_{dref} and zero. This at time $t = 0.2$ ms.

The control of the duty cycle of the chopper enables the output voltage illustrated in Figure 9 to be regulated in a stable mode around 90 V.

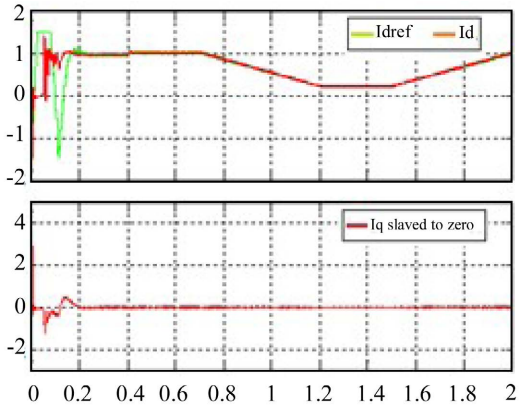

Figure 8. Direct (I_d) and quadratic (I_q) currents after synchronization.

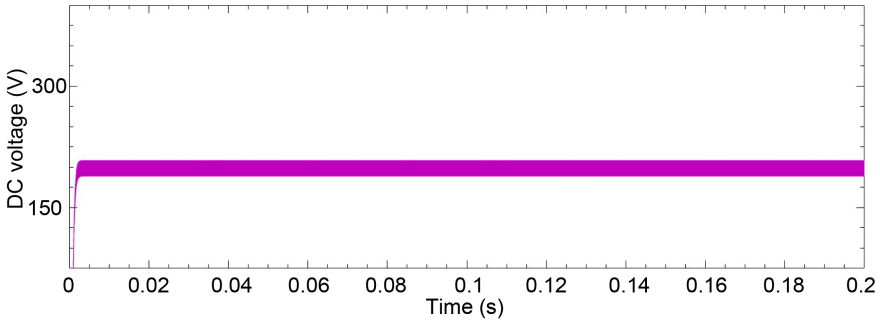

Figure 9. Profile of Boost converter voltage.

The locality of Yagoua has a high solar energy potential. The insolation profile over a 24-hour period is depicted in Figure 10, where, according to climatic data provided by NASA, insolation is close to 1000 W/m^2 as it is depicted in Figure 10.

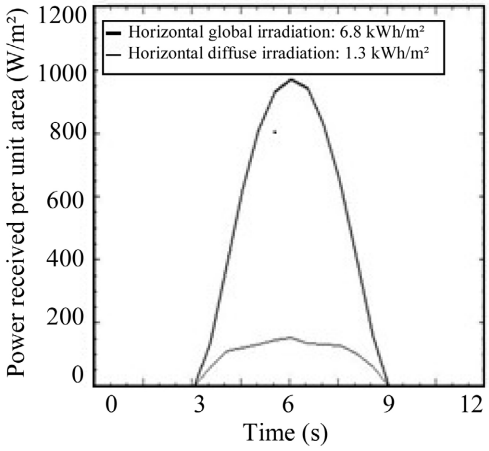

Figure 10. YAGOUA collected data.

In Figure 11, the profile of the load and the energy injected into the electrical network are depicted in Figure 11(a). The correlation between the field temperature is given. Figure 11(b) shows the profile of the energy injected into the power grid. In Figure 11(c), the solar field temperature distribution is determined. In Figure 11(d) we hare humidity profile for different temperatures chosen based on locality conditions.

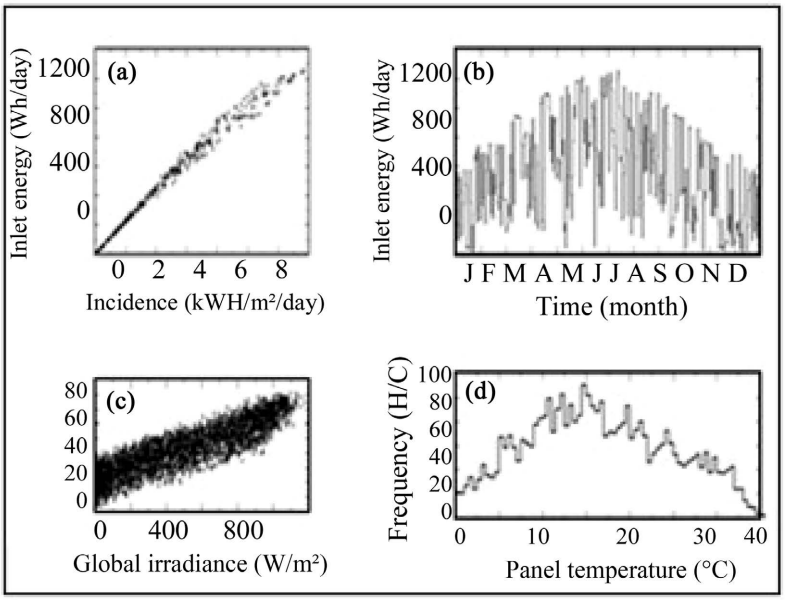

Figure 11. Profile of loads demand.

The energy losses at the inverter level and at the solar array level are calculated using the technico-economic study carried out in the PvSyst software. Under standard conditions, this study shows that a loss of 2.7% is present at the level of the inverters with an efficiency of 2.2% in Figure 12.

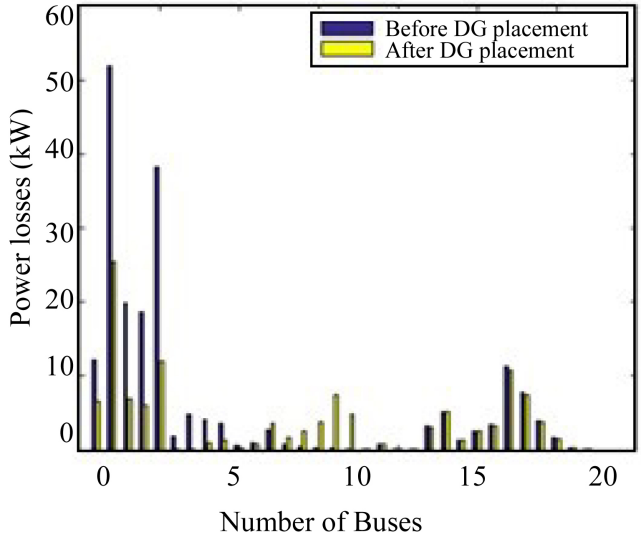

Figure 12. Energy purchased.

Figure 13 depicts the system power losses profile on standard test of IEEE 33 bus. The maximum active power loss is around 52 kW.

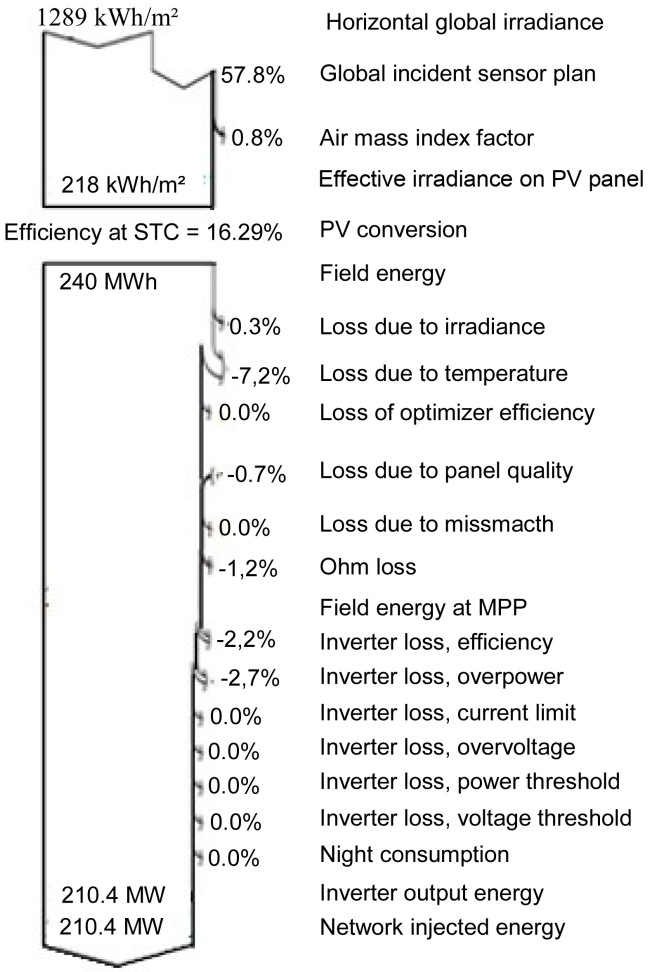

Figure 13. Power loss profile on IEEE 33 bus.

3.2. Shape of the Inverter Output Currents before Filtering

The output currents of the five-level inverters are distorted before filtering and shaping thanks to the model to be studied as depicted in Figure 14.

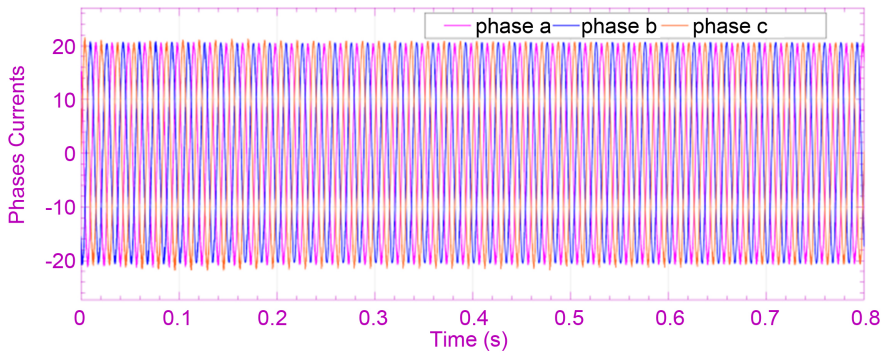

Figure 14. Output currents of three phases before filtering.

For a fundamental of 0.2317, we have a THD = 30.86%, but the control system reduces it as it appears in Figure 15.

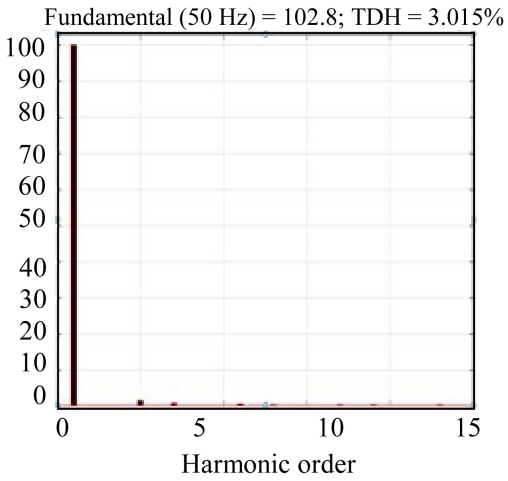

Figure 15. Total harmonic of distortion.

3.3. Shape of the Grid Currents and Voltage after the Inverter Quantities Are Injected

After regulating the electrical quantities from the five-level inverter, we find that after latching, the grid voltages had the same frequency with the output voltages of the five-level inverter; likewise, the output currents are in phase as in Figure 16.

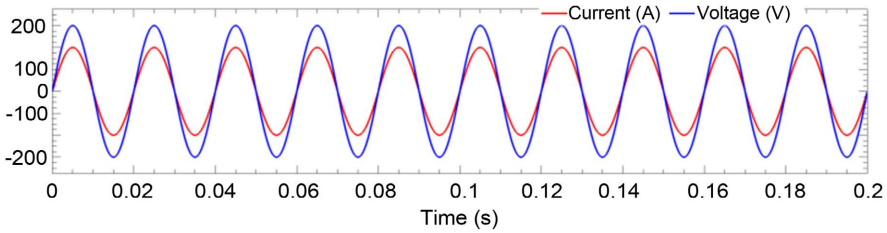

Figure 16. Output current and voltage after filtering for a RL load.

This current is the one we want to control to supply the electrical networks. The three reverse currents of each phase constitute the reference inputs. Figure 17 and Figure 18 depict the currents and voltages profiles of grid and inverter respectively after filtering.

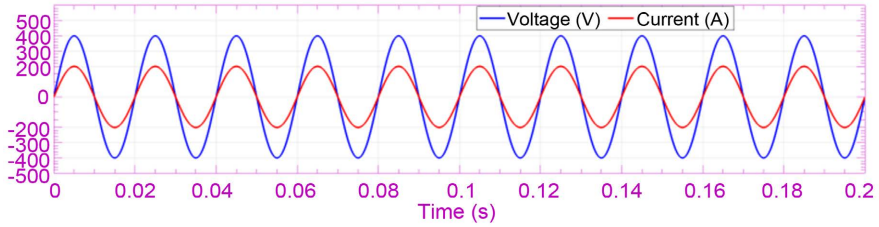

Figure 17. Output current and voltage of the network after filtering.

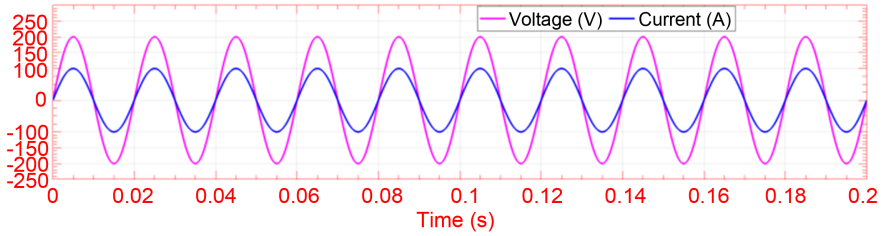

Figure 18. Output current and voltage of the inverter after filtering.

When we use this optimization method, a fundamental of 1094 at 50 Hz gives us a THD = 3.015%. The presence of harmonics in electrical networks is considerably reduced; because a THD of 3.015% for a signal, is so insignificant to be felt or to create a distortion of the current or the voltage. However, before filtering we got a THD = 30.86%.

4. Conclusion

This present work allows firstly to control the duty cycle of the boost chopper thanks to the modified PSO algorithm, secondly to realize a fourth order filter at the output of the chopper through the five-level inverters to see if that can improve the quality of the distorted electrical quantities, resulting from the PVG. After filtering, the output currents of the five-level inverters are injected into the electrical networks thanks to PLL synchronization. This combination of optimization technique has allowed us to improve the cost and efficiency of power flow in power grids. After the simulation results made in Matlab/Simulink and PSIM softwares, we obtained a THD = 3.015%. This technique is found to be interesting for the synchronization of hybrid sources. Unfortunately, during cloudy skies this system is limited as it almost lacks sunlight. Hence there is a need to provide storage batteries or alternative sources. However, the model proposed in this article respects the IEEE standard which allows a THD of 5%, which is much higher than a THD of 3.015% obtained by our proposed model.

Conflicts of Interest

The authors declare no conflict of interest in the publication process of the research article.

References

[1] Meynard, T.A. and Foch, H. (1992) Multi-Level Choppers for High Voltage Applications. *EPE Journal*, **2**, 45-50. https://doi.org/10.1080/09398368.1992.11463285

[2] Schibli, N.P., Nguyen, T. and Rufer, A.C. (1998) A Three-Phase Multilevel Converter for High-Power Induction Motors. *IEEE Transactions on Power Electronics*, **13**, 978-986. https://doi.org/10.1109/63.712325

[3] Manjrekar, M.D. and Lipo, T.A. (1999) A Hybrid Multilevel Inverter Topology for Drive Applications. *IEEE-APEC*'98, Anaheim, 15-19 February 1998, 523-529.

[4] Asiminoaei, L., Blaabjerg, F. and Hansen, S. (2005) Evaluation of Harmonic Detection Methods for Active Power Filter Applications. *The Applied Power Electronics*

Conference (*APEC*), Vol. 1, 635-641.

[5] Nabae, A., Takahashi, I. and Akagi, H. (1981) A New Neutral-Point-Clamped PWM Inverter. *IEEE Transactions on Industry Applications*, **17**, 518-523. https://doi.org/10.1109/tia.1981.4503992

[6] Chenni, R., Matagne, E. and Khennane, M. (2011) Study of Solar Radiation in View of Photovoltaic Systems Optimization. *Smart Grid and Renewable Energy*, **2**, 367-374. https://doi.org/10.4236/sgre.2011.24042

[7] Loschi, H.J., Iano, Y., León, J., Moretti, A., Conte, F.D. and Braga, H. (2015) A Review on Photovoltaic Systems: Mechanisms and Methods for Irradiation Tracking and Prediction. *Smart Grid and Renewable Energy*, **6**, 187-208. https://doi.org/10.4236/sgre.2015.67017

[8] Salas, V., Olías, E., Lázaro, A. and Barrado, A. (2005) New Algorithm Using Only One Variable Measurement Applied to a Maximum Power Point Tracker. *Solar Energy Materials and Solar Cells*, **87**, 675-684. https://doi.org/10.1016/j.solmat.2004.09.019

[9] Bello-Pierre, N., Nisso, N., Kaoga, D.K. and Tchakounté, H. (2023) Energy Efficiency in Periods of Load Shedding and Detrimental Effects of Energy Dependence in the City of Maroua, Cameroon. *Smart Grid and Renewable Energy*, **14**, 61-71. https://doi.org/10.4236/sgre.2023.144004

[10] Roman, E., Alonso, R., Ibanez, P., Elorduizapatarietxe, S. and Goitia, D. (2006) Intelligent PV Module for Grid-Connected PV Systems. *IEEE Transactions on Industrial Electronics*, **53**, 1066-1073. https://doi.org/10.1109/tie.2006.878327

[11] Menzies, R.W., Steimer, P. and Steinke, J.K. (1994) Five-Level GTO Inverters for Large Induction Motor Drives. *IEEE Transactions on Industry Applications*, **30**, 938-944. https://doi.org/10.1109/28.297910

[12] Branbrilla, A., Gambarara, M., Garutti, A. and Ronchi, F. (1999) New Approach to Photovoltaic Arrays Maximum Power Point Tracking. *IEEE Power Electronics Conference* 30*th*, Vol. 2, 632-637.

[13] Kitmo, Tchaya, G.B. and Djongyang, N. (2022) Optimization of Hybrid Grid-Tie Wind Solar Power System for Large-Scale Energy Supply in Cameroon. *International Journal of Energy and Environmental Engineering*, **14**, 777-789. https://doi.org/10.1007/s40095-022-00548-8

[14] Nabipour, M., Razaz, M., Seifossadat, S.G. and Mortazavi, S.S. (2017) A New MPPT Scheme Based on a Novel Fuzzy Approach. *Renewable and Sustainable Energy Reviews*, **74**, 1147-1169. https://doi.org/10.1016/j.rser.2017.02.054

[15] Yaouba, Bajaj, M., Welba, C., Bernard, K., Kitmo, Kamel, S., *et al*. (2022) An Experimental and Case Study on the Evaluation of the Partial Shading Impact on PV Module Performance Operating under the Sudano-Sahelian Climate of Cameroon. *Frontiers in Energy Research*, **10**, Article ID: 924285. https://doi.org/10.3389/fenrg.2022.924285

[16] Song-Manguelle, J., Ekemb, G., Schroder, S., Geyer, T., Nyobe-Yome, J. and Wamkeue, R. (2013) Analytical Expression of Pulsating Torque Harmonics Due to PWM Drives. 2013 *IEEE Energy Conversion Congress and Exposition*, Denver, 15-19 September 2013, 2813-2820. https://doi.org/10.1109/ecce.2013.6647066

[17] Ngoussandou, B., Nisso, N., Kidmo, D.K., Sreelatha, E., Jember, Y.B., Das, S., *et al*. (2023) Optimal Energy Scheduling Method for the North Cameroonian Interconnected Grid in Response to Load Shedding. *Sustainable Energy Research*, **10**, Article No. 14. https://doi.org/10.1186/s40807-023-00084-x

[18] Mounir, B. and Chandra, A. (2012) A New MPPT Algorithm for PMSG Based Grid

Connected Wind Energy System with Power Quality Improvement Features. 5*th IEEE Power India Conference*, Murthal, 19-22 December 2012, 1-6.

[19] Nava-Segura, A. and Carmona-Hernandez, M. (1999) A Detailed Instantaneous Harmonic and Reactive Compensation Analysis of Three-Phase AC/DC Converters, in abc and *αβ* Coordinates. *IEEE Transactions on Power Delivery*, **14**, 1039-1045. https://doi.org/10.1109/61.772351